Int J Thermophys (2008) 29:1156–1165
DOI 10.1007/s10765-008-0401-5

Thermal Noise Sensor Insulation Using Ultra-thin Ceramic Coatings

O. Kerkhof · E. Houtzager · J. v. Wensveen · E. Maloney

Published online: 18 March 2008

Abstract The insulation resistance and interference rejection of several prototype thermal noise sensors were measured. It was found that twisting the connecting wires as a pair optimizes the magnetic interference rejection. High-temperature-resistant wire insulation was developed by vapor depositing a few micrometer thick ceramic coating. The best insulation was obtained with a coating of 1.25 μm SiO_2 + 1.5 μm TiO_2 + 0.25 μm ZrO_2. The insulation of four such coated pairs reached stable levels of 18 ± 3 kΩ during a testing period of 1 week at 950°C under atmospheric conditions.

Keywords Ceramic coating · Insulation resistance · Interference rejection · Noise thermometer · Twisted pair

1 Introduction

Noise thermometry is a method for measuring thermodynamic temperature. Over the past few years, several authors have reported progress in measuring the thermodynamic temperature of various fixed points [1–4]. With respect to uncertainty, noise thermometry has not yet become competitive with other thermodynamic methods, like gas thermometry. Noise thermometry is nevertheless considered useful to check if the various available thermodynamic methods are producing consistent results.

O. Kerkhof (✉) · E. Houtzager
Nederlands Meetinstituut, Van Swinden Laboratorium, Thijsseweg 11, 2629 JA Delft, The Netherlands
e-mail: OKerkhof@NMi.nl

J. v. Wensveen
Tempcontrol Industrial Electronic Products, van Alphenstraat 63s, 2274 NC Voorburg, The Netherlands

E. Maloney
Everest Coatings, Röntgenweg 1, 2624 BD Delft, The Netherlands

Another application of noise thermometry lies in the industrial metrology environment as described previously by Brixy et al. [5,6]. The noise thermometer is unique in the sense that it is independent of sensor drift. Its niche application therefore lies in harsh environments where fast degradation of conventional sensors occurs. In spite of the clear advantages, since the pioneering work of Brixy et al., noise thermometry has not found widespread use in industry. One of the reasons may be the strong electromagnetic fields in industrial environments that can easily overwhelm the small amplitude of the noise signal. Developments in recent years may provide new impetus for the industrial application of the technology. The system developed by FZJ (Forschungszentrum Jülich) in the 1980s and described by Brixy et al. [5] has been upgraded by Zimmermann and Glaas [7]. Consequently, the use of state-of-the-art high-speed electronics, such as digital filters, has decreased the required measuring time. The remaining problem is the sensitivity of the sensor to extraneous noise, i.e., electromagnetic interference (EMI).

This paper describes the first steps made at NMi-VSL to develop a noise sensor for the temperature range up to 1,100°C that is less sensitive to EMI. For this purpose, the well-known twisted-pair technique is used. The innovative aspect lies in the use of thin insulating ceramic layers that enable the use of the sensor at high temperatures while maintaining flexibility for twisting. The insulating and EMI properties of the constructed connecting wires have been investigated and compared with more conventional approaches.

2 Principles of Noise Thermometry

According to the Nyquist theorem, the random movements of charge carriers in a resistor at a finite temperature induce a fluctuating voltage across the ends of that resistor. For the mean square of this voltage, $\overline{V_T^2}$, the following equation holds:

$$\overline{V_T^2} = 4kTR\Delta f \tag{1}$$

where k is the Boltzmann constant, T is the absolute temperature, R is the resistance of the resistor, and Δf is the integration bandwidth. Thus, the absolute temperature of any sensor can, in principle, be determined by measuring the resistance of a sensor element and taking the integrated squared voltage over a certain bandwidth Δf. In practice, the measuring problem is more complicated due to the uncertainty in the transfer function of the signal transmission line. Almost all modern noise thermometers therefore employ the comparison technique pioneered by Dicke [8] in radio astronomy and later applied by Garrison and Lawson [9] in their early noise thermometer design. The technique is based on a comparison of the noise voltages of two resistors to effectively cancel the transmission line transfer function. The temperature to be measured follows from

$$T_S = \frac{\overline{V_S^2}}{\overline{V_R^2}} \frac{R_R}{R_S} T_R \tag{2}$$

where $\overline{V_S^2}$ and $\overline{V_R^2}$ are the mean squared noise voltages across the sensor and a reference resistor, R_R is the resistance of the reference resistor at a known reference temperature T_R, and R_S is the resistance of the sensor at the temperature to be determined. Rapid switching between the sensor and reference resistor eliminates temporal variations in the amplifier gain and frequency response of the thermometer [10].

Still, a large measurement error will result if extraneous noise is superimposed on the useful thermal noise signal. The parasitic noise originates from the sensor leads and amplifiers inside the measuring circuit and from EMI outside the measuring circuit. A correlation technique pioneered by Fink [11] can reduce part of the internally created error. The noise signal from the sensing resistor is fed through two parallel channels. At the end of the double chain, the two signals are multiplied and subsequently averaged. This will result in the cross correlation of uncorrelated signals, like the voltage noise from the leads and amplifiers. The current noise from the amplifiers cannot be eliminated this way. This disturbance must be minimized by optimizing the amplifier design [10]. EMI signals, superimposed on both channels and correlated and usually in-phase, cannot be eliminated by the cross correlation technique. The combination of the comparison and correlation technique was pioneered by Brixy et al. [5].

3 Interference

In a laboratory environment, the presence of EM fields can be reduced significantly by taking certain measures [12]. In the industrial environment, the presence of strong electric and magnetic fields is often a fact of life and one must take measures to reduce their effect on the measurement. Brixy et al. [5,6] have described a number of these measures. Shielding techniques are used to avoid the coupling of external fields into the measuring circuit. Electric fields at low frequencies can be blocked effectively by laying the cables inside conducting metal pipes. Sometimes, ferromagnetic metal pipes are used to provide a degree of screening from magnetic fields. Other well-known techniques to avoid interference from magnetic fields include the use of twisted pairs or coaxial cable.

To avoid ground loops, one should also consider doubly shielded cables and proper grounding. The twisted pair and coaxial cable designs in combination with a differential amplifier having good common-mode rejection further reduce the effect of ground loops. If all measures to prevent interference fail, one can still do two things. Blanking in the time domain will remove interference spikes that occur at a predictable repetition frequency, usually from the electrical mains. If the interferences occur in a limited frequency range, they can be filtered out by implementing hardware band-pass filters or by post processing. In [5], the author reported that the interference problem arises anew with each plant and must therefore be solved individually each time.

The technique that has hitherto not been described in relation to noise sensors is the twisted-pair principle. This is probably because the ceramic material that is used for wire insulation at high temperatures does not lend itself to twisting. The authors of this paper investigated the feasibility of twisting high-temperature sensor leads insulation with an ultra-thin ceramic coating.

4 Sensor Design

It is well known that twisting a pair of wires reduces the loop area between the wires, and thereby the magnetic coupling, in a direct way. Furthermore, the induced noise in one loop is cancelled out by the induced noise in the successive loop. The noise rejection thus gets better for more tightly twisted pairs, especially if the EM field is non-uniform. At high temperatures, however, ceramics are the insulating material of choice and their mechanical properties would seem to prevent the application of the twisted-pair technique. However, this does not necessarily have to be the case. Mineral-insulated cables contain a densely packed ceramic powder that allows some bending. In fact, to make the metal sheath of mineral-insulated cables more rigid, it is sometimes work-hardened by twisting it lightly.

Two probes were made from four-wire mineral-insulated cable (Ni wires with thickness 0.51 mm, insulated with Al_2O_3 ceramic powder, Inconel 600 sheathing, outer diameter 6 mm). One probe was twisted by heating the cable and applying a torque on one side of the cable while fixing the other end (see Fig. 1a). The number of twists thus obtained was four twists over a length of 50 cm. Two other probes were made out of two 2-wire mineral-insulated cables (Ni wires with thickness 0.30 mm, insulated with Al_2O_3 ceramic powder, Ni sheathing, outer diameter 2 mm). For one of the probes, the two mineral-insulated cables were twisted as a pair (12 twists over a length of 50 cm) as shown in Fig. 1b. These two probes were also equipped with a wire-wound industrial PT-25 element.

Although the mineral-insulated and sheathed cables allow some bending and twisting, the tightness and number of twists are very limited. Therefore, we investigated the possibility of combining the wear resistance of ceramics with the bendability of metals. Type-N thermocouple wires were coated by a vapor deposition technique with ultra-thin ceramic layers to obtain a high-temperature-resistant insulation while maintaining wire flexibility. After initial testing using single, dual, and triple layers, it was decided to continue with triple layers of SiO_2, TiO_2, and ZrO_2. The SiO_2 layer is the main contributor to the electrical insulation. The SiO_2 layer is, however, likely to crack and/or delaminate from the wires due to differential thermal expansion with respect to the wire. The second layer of TiO_2 has a much higher expansion coefficient and is supposed to hold the SiO_2 together. The ZrO_2 is applied on top to avoid oxygen transport through the TiO_2 at elevated temperatures.

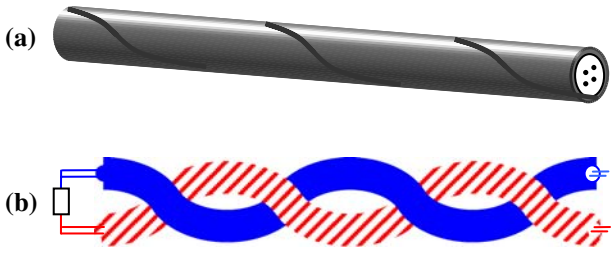

Fig. 1 (**a**) Four-wire mineral-insulated cable twisted by applying a torque and (**b**) 2 × 2-wire mineral-insulated cables twisted as a pair

The thickness of the individual layers was varied, and for each configuration, a set of four pairs was manufactured. It was expected that the very thin ceramic layer could not provide superior electrical insulation. The following section explains that this will nevertheless lead to modest errors in the case of industrial application.

5 Insulation Resistance

It is generally known that insulation resistances rapidly decrease at high temperature. In principle, this causes a signal loss. At the same time, the parasitic insulation resistance causes an additional noise current to be injected into the signal line. Moreover, the noise current induced in the line resistance is not completely cancelled by the cross correlation since it couples into the other signal line through the low insulation resistance. The total measured noise signal is then a superposition of these contributions, as shown in Fig. 2. The measured resistance is, however, equal to the combination of the same resistances as shown in Fig. 2. As long as the temperature of the sensor and the measuring cable are the same, no error occurs and the measuring sensor can be regarded as distributed over the length of the cable. In practice, the temperature distribution will not be uniform in the hot zone. We consider the general situation whereby both the sensor resistance R_s with corresponding noise voltage v_s and the insulation resistance R_i with corresponding noise voltage v_i contribute to the total measured noise voltage v_m:

$$v_m = \frac{R_i}{R_s + R_i} v_s + \frac{R_s}{R_s + R_i} v_i \tag{3}$$

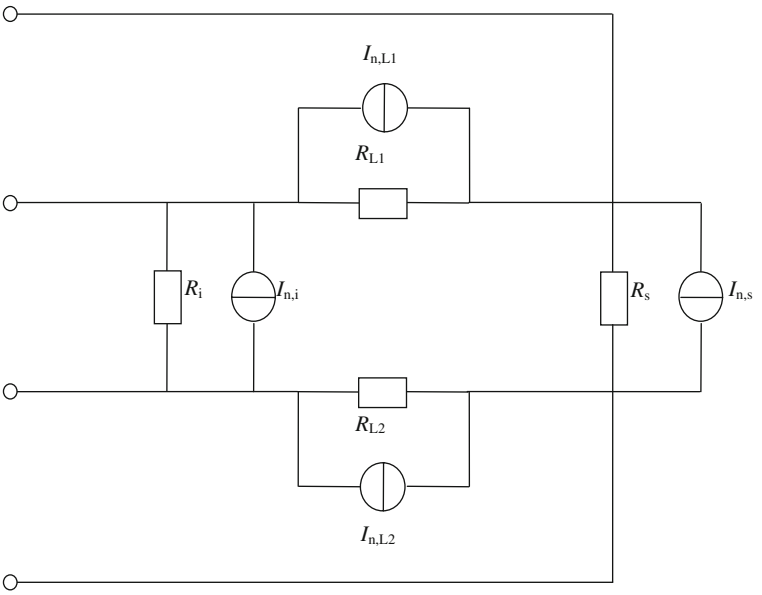

Fig. 2 Equivalent diagram showing the noise contributions of the sensor and leads

The measured resistance R_m equals $R_s // R_i$

$$R_m = R_s \frac{R_i}{R_s + R_i} \tag{4}$$

The calculated temperature then equals

$$T_{calc} = \frac{\bar{v}_m^2}{4kR_m\Delta f} = \frac{R_i}{R_s + R_i} T_s + \frac{R_s}{R_s + R_i} T_i \tag{5}$$

If the temperatures of the sensor T_s and insulation T_i are the same, no error is made. If the temperatures are not the same, an error will result that will be a maximum (theoretically) when $T_i = 0$. In that case, an insulation resistance that is only 100 times higher than the sensor resistance leads to a maximum error of about 1%.

In practice, the error is smaller, as was experimentally determined by Brixy in a temperature gradient field. The measuring sensor was first positioned at the temperature maximum and, later on, beyond the temperature maximum in a colder zone. In the latter case, a ratio of the insulation resistance to the sensor resistance of 10 proved to be sufficient to keep the error under 0.5%. In the first case, the ratio needed to be only six to keep the error under 0.5%. It appears that the insulation is less critical than one might expect.

6 Results

We have determined the insulation resistances as well as the interference rejection properties of various probes. The aim was to obtain a sufficiently high insulation resistance while optimizing interference rejection.

6.1 Insulation Resistance Tests

Directly after twisting the 2 × 2-wire cable, the insulation resistance dropped from 60 MΩ to 200 kΩ, at 400°C. After heating at 1,000°C for a few hours, the insulation was restored. The same happened after twisting the coated pairs at room temperature, which sometimes resulted in an insulation resistance of only a few ohms. After heating at 950°C for some time, the insulation resistance recovered.

The insulation resistance was determined using a current source (Keithley 263) and measuring the voltage with a digital multimeter (DMM) (HP 34420A). For the coated pairs, the insulation resistances decreased between 20% and 50% when the current was increased from 20 µA to 100 µA. The noise thermometer's built-in DMM applies a current of 0.25 mA, which implies that only a few microamperes will go through the insulation layer. The reported insulation resistances in Table 1 are therefore calculated at low current levels. The insulation resistance of the four-wire mineral-insulated cables was about 20 kΩ at 950°C. The insulation resistance of the 2 × 2-wire mineral-insulated cable was of the same order for the untwisted probe and was only 1 kΩ at 950°C for the twisted probe.

Table 1 Insulation resistance of various test probes at high temperature

Probe	Description	R_{iso} (kΩ) $T = 950°C$ $t < 24\,h$	R_{iso} (kΩ) $T = 950°C$ $t > 48\,h$	R_{iso} (kΩ) $T = 950°C$ $t > 100\,h$
MIC-4-U	4-Wire mineral-insulated cable untwisted	20	–	–
MIC-4-T	4-Wire mineral-insulated cable twisted	22	–	–
MIC-2-2-U	2 × 2-Wire mineral-insulated cable untwisted	24	–	–
MIC-2-2-T	2 × 2-Wire mineral-insulated cable twisted	2	–	–
N1-T	1.00 µm SiO_2 + 1.50 µm TiO_2 + 0.25 µm ZrO_2	–	5.2 ± 1.8	5.5 ± 1.4
N2-T	1.00 µm SiO_2 + 1.25 µm TiO_2 + 0.25 µm ZrO_2	8.0 ± 1.8	7.1 ± 2.9	–
N3-T	1.25 µm SiO_2 + 1.50 µm TiO_2 + 0.25 µm ZrO_2	24.9 ± 30.8	17.2 ± 4.4	18.1 ± 2.6
N4-T	1.25 µm SiO_2 + 1.25 µm TiO_2 + 0.25 µm ZrO_2	–	2.9 ± 1.9	5.9 ± 1.8
N5-T	1.00 µm SiO_2 + 0.25 µm ZrO_2 + 1.25 µm TiO_2	4.1 ± 2.6	–	3.2 ± 1.5

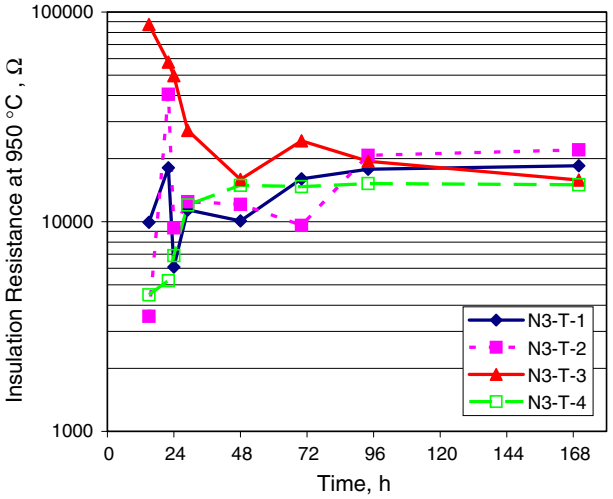

Fig. 3 Insulation resistance of a coated (1.25 µm SiO_2 + 1.5 µm TiO_2 + 0.25 µm ZrO_2) and twisted Type-N thermocouple pair as a function of time

The results for the coated Type-N wires are presented as averages plus standard deviations of four identical pairs. The insulation resistance of the coated and twisted Type-N thermocouple pairs varied between 3 and 80 kΩ at 950°C. The combination of 1.25 µm SiO_2 + 1.5 µm TiO_2 + 0.25 µm ZrO_2 provided the highest insulation resistance.

The time-dependent insulation resistance of the N3-T pairs is shown in Fig. 3. In the first 24 h, the variation is between 4 and 80 kΩ at 950°C. The variation decreased after a couple of days with insulation resistances of 18 ± 3 kΩ. In general, we applied about 10 twists over a length of 50 cm. For probe N4-T, the number of twists was varied between 10 (N4-T-1) and 18 (N4-T-4) twists per 50 cm. Both pairs exhibited the same insulation resistance of 4.5 kΩ at 950°C.

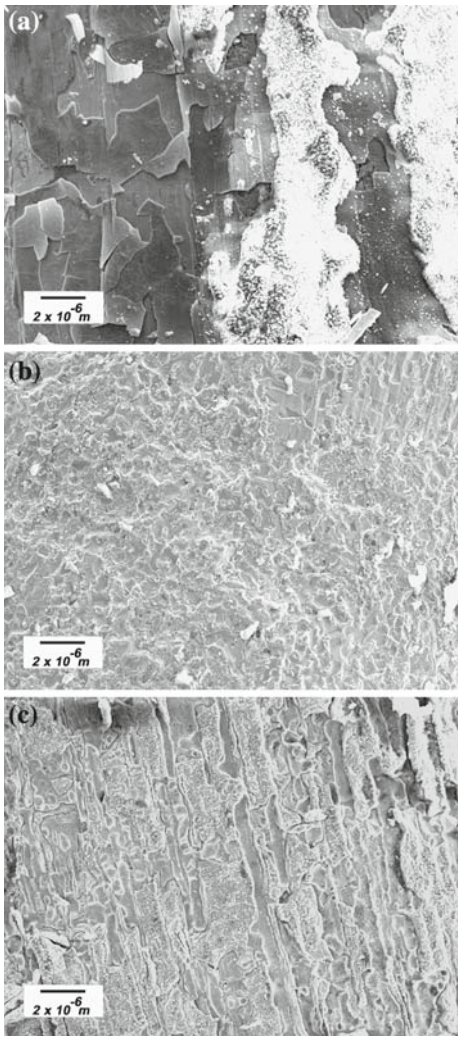

Fig. 4 SEM micrographs of coated wires; magnification: 500x; Acc. Voltage: 15 kV: (**a**) partly delaminated coating after twisting, (**b**) typical surface morphology of a coated negative wire after prolonged exposure to air at 950°C, and (**c**) typical surface morphology of a coated positive wire after prolonged exposure to air at 950°C

In particular, the thermally processed positive lead (Ni, Cr 14.2%, Si 1.4%) looked damaged based on visual inspection. The coated wires were studied with a JEOL-5800 scanning electron microscope (SEM). Figure 4a shows the morphology of a positive lead after twisting. As can be seen, due to the mechanical loading, the coating has partially delaminated. The white crystals on the right side are presumably thick oxides (which are non-conducting and appear white in a SEM) grown from within the wire, during the coating process. Figure 4b shows the surface morphology of a negative lead (Ni, Si 4.4%, Mg 0.1%) after prolonged exposure to air at 950°C. Figure 4c shows the surface morphology of a positive wire after prolonged exposure to air at 950°C. In this case, it seems that part of the coating has become fluid.

6.2 Electromagnetic Interference Rejection

The mineral-insulated probes were investigated for their ability to reject magnetic interference. This represents the biggest challenge when comparing EM fields and purely electric fields. A calculable alternating magnetic field of about 1 mT was realized in the center of a Helmholtz coil. This field is calculable by means of the equation,

$$B = \left(\frac{4}{5}\right)^{3/2} \frac{\mu_0 n I}{R} \tag{6}$$

B is the magnetic field in the center of the Helmholtz coil, μ_0 is the permeability constant ($= 4\pi \times 10^{-7}\,\mathrm{T \cdot m \cdot A^{-1}}$), n is the number of turns, I is the coil current, and R is the coil radius. We applied 300 mA through a coil with a radius of 1 cm and a total of 20 turns and inserted the probes along the coil axis. A lock-in amplifier (SRS SR830) was used to measure the interference signal in the frequency range between 1 and 100 kHz. The twisted and untwisted mineral-insulated cables, in general, exhibited higher magnetic interference signals than the unshielded pairs. The effect of twisting was clearly seen for two pairs of unshielded and Teflon-insulated wires. The twisting (170 twists per meter) resulted in a reduction of interference by a factor of 10. Two pairs of coated and twisted N-type wires were tested with 18 and 10 twists, respectively, over a length of 50 cm. The more tightly twisted pair exhibited a factor of three greater reduction in magnetic interference.

7 Discussion

Various connection wire configurations have been tested for insulation resistance and magnetic interference properties. Most surprisingly, the wires with a 3-µm-thick ceramic coating exhibited rather high insulation resistances, comparable to or better than the mineral-insulated cables. It may seem obvious that the thickest coating (1.25 µm SiO_2 + 1.5 µm TiO_2 + 0.25 µm ZrO_2) has the highest insulation resistance of about 18 kΩ. However, one must bear in mind that a thicker layer will be less flexible and tolerant against twisting and may actually result in more severe breakage of the insulation. From the SEM micrographs and the insulation resistance measurements, it seems that at high temperature the cracks are filled by new oxides and by fluidization of the insulating material causing the formation of a closed layer. The ceramic layer thus appears to be self-healing.

The insulation resistance appears to be stable over time. Apparently, the especially mobile Cr atoms in the positive wires do not destroy the ceramic coating. This may be an indication of thermodynamic equilibrium between the ceramic coating and the wire. We must obtain more insight into these processes by energy dispersive diffractive X-ray spectrometry (EDX).

The effect of twisting was clearly observed for the unshielded Teflon or ceramic-insulated wires. The shielded mineral-insulated cables did not provide substantial interference rejection compared to the unsheathed cables. This may be because the

former have a tighter twist and smaller loop area compared to the mineral-insulated cables. Apparently, the screening itself was not effective and deserves better attention.

A sheathing made from ferromagnetic material should also provide additional reduction of magnetic interference. The sheathing of the MIC-2-2 (Ni sheathing) and the MIC-4 (Inconel 600 sheathing) probes do possess ferromagnetic properties. We were unable to demonstrate that this provides effective screening. Another point of attention is that the ferromagnetic properties will be lost at high temperatures beyond the Curie temperature, T_C. A sheath made out of cobalt foil ($T_C = 1{,}121°C$) may overcome this problem.

8 Conclusion

Recent studies at NMi-VSL demonstrate the feasibility of developing noise sensors with the hot part of the connection leads configured as a twisted pair. A rather high and stable insulation resistance of about 18 kΩ at 950°C was obtained for twisted N-type thermocouple wires that were coated with a multi-layer of 1.25 µm SiO_2 + 1.5 µm TiO_2 + 0.25 µm ZrO_2. The combination of a noise sensor element of about 100Ω and this finite insulation resistance should result in a relatively small error <0.1%. This remains to be investigated in practice. The ceramic coating appears to be self-healing to some extent. The nature of this process will be the topic of further research using both SEM and EDX analysis.

The advantage of the thin coating is the possibility to produce a tightly twisted pair. This appears so far to be the most effective measure to reduce magnetic interference. The effect of sheathing on electromagnetic field interference will also be a topic of further research.

References

1. D.R. White, R.S. Mason, P. Saunders, in *Proceedings of TEMPMEKO 2001, 8th International Symposium on Temperature and Thermal Measurements in Industry and Science*, ed. by B. Fellmuth, J. Seidel, G. Scholz (VDE Verlag, Berlin, 2002), pp. 129–134
2. M.J. de Groot, J.F. Dubbeldam, H. Brixy, F. Edler, E. Tegeler, Noise thermometry measurements at fixed points. CCT document CCT/96-30 (1996)
3. F. Edler, M. Kühne, E. Tegeler, Metrologia **41**, 47 (2004)
4. J.T. Zhang, S. Xue, Metrologia **43**, 273 (2006)
5. H. Brixy, R. Hecker. K.F. Rittinghaus, H. Höwener, in *Temperature: Its Measurement and Control in Science and Industry*, vol. 6, Part 2, ed. by J.F. Schooley (AIP, New York, 1982), pp. 1225–1237
6. H. Brixy, in *Sensors, A Comprehensive Survey*, vol. 4, *Thermal Sensors* (VCH Verlagsgesellschaft, Weinheim, 1991), pp. 225–251
7. E. Zimmermann, W. Glaas, *Rauschthermometer Typ 6*, Interner bericht des Forschungszentrums Jülich, KFA-ZEL-IB-500399 (June 1999)
8. R. Dicke, Rev. Sci. Instrum. **17**, 268 (1946)
9. J.B. Garrison, A.W. Lawson, Rev. Sci. Instrum. **20**, 785 (1949)
10. D.R. White, E. Zimmermann, Metrologia **37**, 11 (2000)
11. H. Fink, Can. J. Phys. **37**, 1397 (1959)
12. D.R. White, R.S. Mason, P. Saunders, in *Proceedings of TEMPMEKO 2004, 9th International Symposium on Temperature and Thermal Measurements in Industry and Science*, ed. by D. Zvizdić, L.G. Bermanec, T. Veliki, T. Stašić (FSB/LPM, Zagreb, Croatia, 2004), pp. 485–490